

Simulating a magnetized bead pile

Thomas F. Gilliss

Physics Department, The College of Wooster, Wooster, Ohio 44691, USA

(Dated: May 10, 2012)

A computer simulation was written to explore the dynamics of a two-dimensional, monodisperse system of spherical particles. By treating beads as distinct elements, a phenomenological representation of the Bak, Tang and Wiesenfeld pile was obtained, allowing for a more in depth interaction with pile dynamics than would many cellular automaton models. A pile was built by dropping beads randomly onto a base, and the relationships between simulated forces determined angle of repose and avalanche behavior. A magnetic field was successful in adding cohesion amongst the beads, which were treated as single dipoles, and chains were observed to form within the pile along the direction of lowest energy dipole orientations. Data suggested power law behavior in the distribution of avalanche sizes, where about 86% of all avalanches were of the smallest sizes, and less than 0.1% of avalanches were of 10 beads or more. Avalanche distributions are expected to increasingly differ from this power law behavior as the magnetic field strength increases. Data runs were taken at low magnetic field strengths, in trials consisting of 10 000 bead drops.

PACS numbers: 45.70.-n, 05.65.+b, 45.70.Ht

INTRODUCTION

A pile of granular materials is a complex, many-bodied system that exhibits stochastic behavior in its cycles of building and falling. When an element is added to the pile, the disturbance dissipates a force through the existing pile. The resulting system of short range interactions propagates in complex paths and determines the resting place of the particle. This stability represents a minimally stable state—a point at which the force could propagate no further.

Over the course of many grain additions, the pile builds to a critical angle of repose. At this point, the pile can exhibit a wide range of effects as a result of only a slight perturbation. For example, any further grain additions to the critical pile will bring the slope to a supercritical critical state and cause avalanches of a range of sizes.

Critical systems are said to exhibit self-organized criticality if they approach a critical point without dependence on tuning parameters. A granular pile is an example of such a system, approaching its minimally stable critical angle regardless of tuning parameters. In addition to this “sandpile”, Bak, Tang, and Wiesenfeld (BTW) proposed that a multitude of other systems, including the formation of fractal patterns in nature, self-organize toward critical points [1]. Further research into self-organized criticality has suggested that the same principles govern the behavior of earthquakes, the propagation of forest fires, motor traffic, and fluctuations in the stock market [2].

Research at The College of Wooster has tested a number of parameters and how they affect the avalanche behavior of a pile of spherical steel beads, where the beads serve as an idealized sandpile. In changing the region and height of bead drops, deviations in the probabilities of avalanches have been observed. These effects can be

seen in Fig. 1 where the avalanche size distribution systematically rolls off from pure power law behavior.

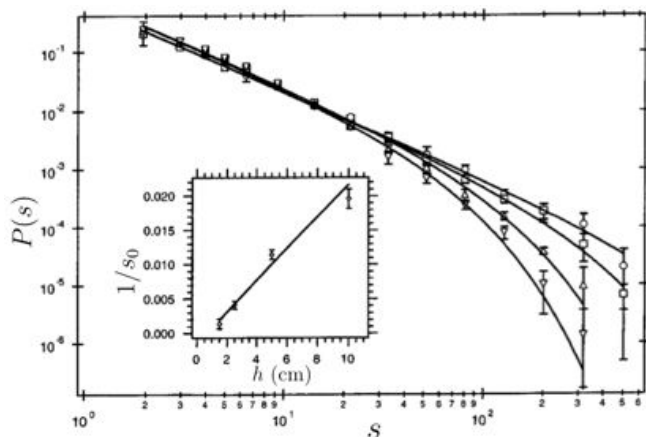


FIG. 1: Avalanche probability versus size. As the drop height increases, over four trials, roll off from power law behavior becomes more prominent. The inset figure displays characteristic avalanche sizes—the points at which data begins to deviate from a pure power law—against drop height. The exponent τ of the power law fit was measured as 1.47 ± 0.03 [3].

Altering the cohesion between the beads has also been shown to cause deviation from power law behavior. By placing the pile within a magnetic field, a magnetic interparticle force arises and causes cohesion between the beads [4].

Researchers at The College of Wooster magnetized steel beads by placing them within a pair of Helmholtz coils. As suspected, clustering within the pile developed into vertical chains, and groups of beads became somewhat resistant to forces propagating through the pile. These effects led to a decrease in the probability of medium sized avalanches and an increase in the size and probability of large avalanches.

Our simulation tests the affects of magnetic fields on pile behavior and allows experiments to control such parameters as air viscosity, drop height, and the material properties of the beads. The ability to alter these parameters, along with the convenience of the speed of computation, gives our simulation an advantage over experimental methods, where data runs of 20 000 bead drops take 54 hours to complete [5].

THEORY

Power Law Behavior

The wide range of length and time scales over which critical behavior occurs can be modeled by a pure power law describing the presence of a large probability of small events and a smaller probability of large events. Accordingly, the probability of an avalanche of size s in the bead pile is

$$P(s) = P_0 s^{-\tau}, \quad (1)$$

where τ is an exponent. Mean-field models find τ to have a value of 1.5 [3].

Magnetic Dipole Interactions

The magnetic field strength \vec{B} of a dipole in free space, with permeability μ_0 , can be modeled by

$$\vec{B} = \frac{\mu_0}{4\pi} \frac{3\hat{r}\vec{m} \cdot \hat{r} - \vec{m}}{r^3}, \quad (2)$$

where \vec{m} is the magnetic moment and r denotes the distance between poles. The direction of the field, represented by vectors pointing from the positive to negative pole, can be seen in Fig. 2.

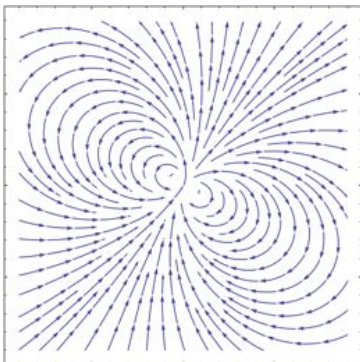


FIG. 2: The magnetic field lines of a dipole. The density of field lines corresponds to the strength of the field.

When the dipole is exposed to an external magnetic field, the potential energy U of the system is described

by the scalar product

$$U = -\vec{m} \cdot \vec{B}_2, \quad (3)$$

where \vec{B}_2 represents the external magnetic field. The force applied to the dipole then goes as the opposite of the gradient of the energy

$$\vec{F} = -\vec{\nabla}U. \quad (4)$$

For a system with two identical and vertically oriented dipoles $\vec{m}_1 = \vec{m}_2 = m$, the expression for the force can be written in terms of its x and y components. In the x direction,

$$F_x = \frac{\mu_0}{4\pi} \frac{3m^2}{\delta r^7} \delta x (\delta x^2 - 4\delta y^2). \quad (5)$$

And in the y direction,

$$F_y = \frac{\mu_0}{4\pi} \frac{3m^2}{\delta r^7} \delta y (3\delta x^2 - 2\delta y^2). \quad (6)$$

The variables δx , δy , and δr represent the component and total distances between the dipoles.

It is convenient to group the constants out front of Eqns. 5 and 6, defining a single constant M as

$$M \equiv \frac{\mu_0}{4\pi} 3m^2. \quad (7)$$

SIMULATION METHOD

The computer simulation, coded in Obj-C/C++, is based on a two-dimensional, distinct element method similar to that of Fazekas, Kertész, and Wolf [6]. To study avalanche behavior as it depends on a number of pile parameters, we implement forces governing collisions, magnetic interactions, gravity and air viscosity, and the internal friction of the beads.

Beads are stored in an array whose width is the maximum number of beads. To update the interactions and positions of the beads, the net force on each is divided by the mass of the bead and converted to an acceleration, according to Newton's Second Law. An Euler-Cromer algorithm then numerically integrates, converting accelerations to velocities, and then to positions. For the x components, this method takes the form of

$$v_x \leftarrow v_x + a_x dt, \quad (8a)$$

$$r_x \leftarrow r_x + v_x dt. \quad (8b)$$

A similar method for the y components goes as

$$v_y \leftarrow v_y + a_y dt, \quad (9a)$$

$$r_y \leftarrow r_y + v_y dt. \quad (9b)$$

The position of the bead, here, is r , and dt , the integration time step. The time is incremented by dt using the statement $t \leftarrow t + dt$. A typical value for dt was 0.001 s.

The contact force is modeled to limit the ability of beads to overlap. As δr between two beads approaches the radius of a bead R , the magnitude of the contact force reaches an asymptotic limit and the position r of a bead cannot come any closer. The contact force was modeled as

$$F_c = \alpha \frac{(\delta r - R)^2}{\delta r}, \quad (10)$$

where α is a constant adjusting the strength of the force.

The force of gravity was modeled simply as $\vec{F}_g = -m\vec{g}$ where m is the mass of a bead, and $\vec{g} = 9.8 \text{ m/s}^2$. \vec{F}_g was countered by a ground force \vec{F}_b which shared a similar shape to \vec{F}_c and insured that beads did not pass through the pile's base. The base was made sticky so that an initial layer of beads could form.

We implemented viscosity and friction for numerical stability. The force due to the viscosity of air was modeled as $\vec{F}_v = -\gamma\vec{v}$, where γ is a strength coefficient. \vec{F}_v always opposed the direction of motion, and was usually relatively weak with $\gamma < 1$. For the frictional force \vec{F}_f , we represented the deformation of beads under stress as

$$\vec{F}_f = -\mu\hat{v}F_b. \quad (11)$$

\vec{F}_f , here, effectively depends on the distance between two objects [7]. The strength coefficient μ is usually initialized as 0.50.

To achieve the effect of magnetization in the pile, the beads are treated as single dipoles, all of which are parallel to a uniform magnetic field running vertically. The identical dipoles present a special case, as previously mentioned, and the x and y components are calculated separately using Eqns. 5 and 6.

Comparing Eqns. 5 and 6, notice that interacting dipoles will achieve a lowest energy state when aligned head-to-tail. Given the vertical orientation of our dipoles, head-to-tail alignment occurs at $\delta x = 0$ and yields a magnetic force, purely in the y direction, of

$$F_y = \frac{-2M}{\delta y^4}. \quad (12)$$

This configuration is the energetically most favorable state, and consequently, beads tend to form vertical chains within the pile [6]. The relationship of δx and δy to the magnetic force in the vertical direction can be seen in Fig. 3.

A double “for” loop cycled through every potential bead-bead interaction when calculating the contact and magnetic forces. As the magnetic force acts at a distance, and cycling through every bead combination would be inefficient, we employed a cutoff distance for the checking of magnetic interactions. This distance was 6 times the diameter of a bead, a value that maintains the realism of magnetic clustering behavior and changes the magnetic energy per particle by less than 5% [8].

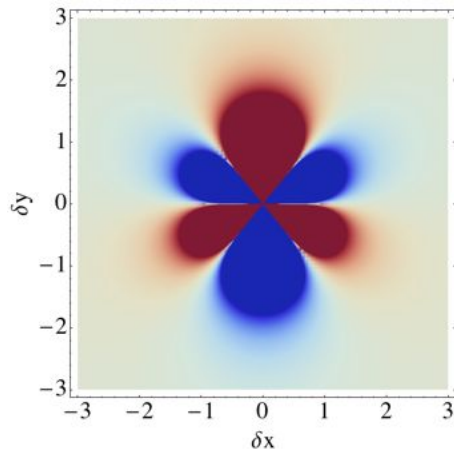


FIG. 3: The magnetic force in the y direction plotted against various dipole orientations. The darkening range of red colors indicates increasingly negative values of F_y , while the range of blues indicates increasingly positive values of F_y . Notice that F_y approaches negative infinity as the dipoles approach the lowest possible energy alignment.

In order to let avalanches run their course without the interference of dropping beads, the total kinetic energy of the system is monitored. The next bead is only dropped if the pile's kinetic energy has fallen below a certain point, indicating that the beads have settled and any avalanches have ended.

When a new bead is dropped onto the pile, there is potential for an avalanche of a wide range of sizes to occur. To record the size of avalanches, we increment a counting variable for each bead that leaves the width of the pile and falls below the origin. We allow beads to fall off both sides of the pile. The avalanche count is continued for each bead that leaves the pile until K approaches 0 and the next bead is dropped. At this point, the counting variable is cleared and made available to tally the avalanche size for the life time of the next bead drop.

An experiment mode was included to take avalanche data over a large number of bead drops. This option bypassed the drawing routine and sped up the simulation speed so that a large number of data points could be collected quickly. Using print statements, the initial conditions for the trial, avalanche sizes, and number of bead drops were recorded to be used for analysis.

RESULTS

The simulation was successful in emulating the multitude of short range forces governing granular systems in nature. Given initial conditions, bead after bead would fall, piling on top of one another until a pile similar to that of Fig. 4 was formed. Small values for γ and μ allowed the beads to bounce more, taking longer to dissi-

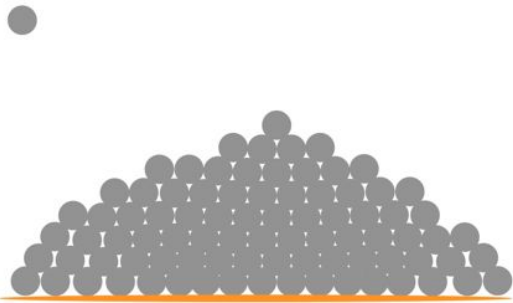


FIG. 4: A typical pile. The random arrangement of the base layer played a large role in the dynamics of small piles.

pate their energy. High values for κ and α made bead interactions more rigid and allowed the pile to build higher.

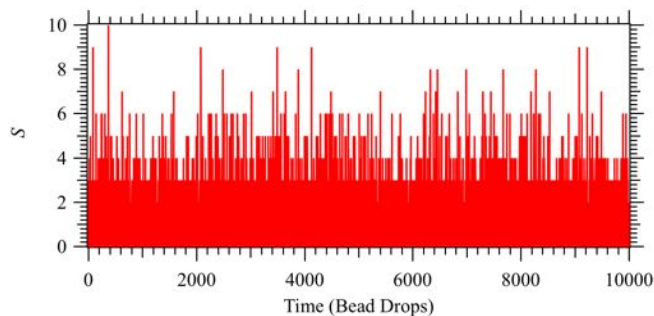


FIG. 5: Avalanche size versus time for the $M = 0 \text{ N} \cdot \text{mm}^4$ trial. The large number of occurrences of small avalanches relative to the low frequency of large avalanches is shown well here.

To investigate the effect of the magnetic field, two initial runs of 10 000 bead drops were completed. These two runs, at $M = 0 \text{ N} \cdot \text{mm}^4$ and $M = 20 \text{ N} \cdot \text{mm}^4$, showed little difference in avalanche behavior despite their differences in magnetic field strength.

The first trial was run without a magnetic field and the data was analyzed using Igor Pro. Viewing an avalanche size versus time plot, shown in Fig. 5, indicates that most avalanches were comprised of a single bead, and that increasingly large avalanches were increasingly rare. This power law behavior, where the probability of small events is large and that of large events is small, is confirmed when the fractional occurrence of average avalanche sizes is calculated. For the $M = 0 \text{ N} \cdot \text{mm}^4$ run, 1-2 bead avalanches took up $85.8 \pm 0.1\%$ of the total number of avalanches. 3-4 bead avalanches made up $11.6 \pm 0.1\%$ of the total. Following the downward trend, $2.2 \pm 0.1\%$ were 5-6 bead avalanches, and $0.35 \pm 0.1\%$ were of 7-8 beads. Finally, avalanches of 10 beads or more comprised of only $0.1 \pm 0.1\%$ of the total.

The similarity between the $20 \text{ N} \cdot \text{mm}^4$ and $0 \text{ N} \cdot \text{mm}^4$ runs was due to the magnetic field being far too weak. As it turns out, noticeable cohesion amongst the beads

only occurs with $M \geq 100\,000 \text{ N} \cdot \text{mm}^4$, corresponding to a magnetic dipole moment of $0.577 \text{ A} \cdot \text{m}^2$. Above $100\,000 \text{ N} \cdot \text{mm}^4$, beads can be seen aligning into the predicted chain formations.

CONCLUSION

A two-dimensional, monodisperse pile of magnetizable beads is capable of modeling the behavior of granular systems in the presence and absence of magnetic fields. Our simulation's adjustable parameters also make it possible to emulate beads of various coefficients of restitution, and piles of various geometries. As seen in the plots of probability versus average avalanche size, and confirmed by work in similar studies, the distribution of avalanche sizes follows power law behavior indicative of self-organized criticality. In addition, the unpredictability of avalanche sizes in time confirms the simulation's ability to build a pile to its critical point.

The addition of a magnetic field successfully produces cohesion between the beads, but is yet to be tested over large numbers of bead drops. Based on the experimental and computational results of other research groups, we expect trials with increasing field strengths to yield avalanche size distributions with systematic roll off from pure power law behavior. In addition, increases in the size and probability of large avalanches should occur, appearing as second humps in the distributions of avalanche sizes [5, 6, 9].

Future work at The College of Wooster can improve this simulation by increasing processing speed and taking the simulation into three dimensions where new geometry within the system can affect pile dynamics.

ACKNOWLEDGEMENTS

I sincerely thank John Lindner for much help and discussion, and for calling my attention to certain papers.

-
- [1] P. Bak, C. Tang, and K. Wiesenfeld, *Phys. Rev. Lett.*, **59**, 381 (1987).
 - [2] D. L. Turcotte, *Rep. Prog. Phys.*, **62**, 1377-1429 (1999).
 - [3] D. T. Jacobs *et al.*, *Phys. Rev. E*, **67**, 041304 (2003).
 - [4] F. Peters and E. Lemaire, *Phys. Rev. E*, **69**, 061302 (2004).
 - [5] T. F. Gilliss, *The College of Wooster*, 1 (2011).
 - [6] S. Fazekas, J. Kertész, and D. E. Wolf, *Phys. Rev. E*, **71**, 061303 (2005).
 - [7] S. Luding, *The Physics of Granular Materials*, edited by H. Hinrichsen and D. E. Wolf (Wiley-VCH, Weinheim, 2004).
 - [8] S. Fazekas, J. Kertész, and D. E. Wolf, *Phys. Rev. E*, **68**, 041102 (2003).
 - [9] Volkhard Buchholtz *et al.*, *J. Stat. Phys.*, **84**, 1373 (1996).